

**E. Huschek-Juhász**<sup>1</sup>,  
orcid.org/0000-0002-5544-3146,  
**A. Németh**<sup>1</sup>,  
orcid.org/0000-0002-3477-6902,  
**M. Sysyn**<sup>2</sup>,  
orcid.org/0000-0001-6893-0018,  
**G. Baranyai**<sup>1</sup>,  
orcid.org/0000-0003-3369-8823,  
**J. Liu**<sup>3</sup>,  
orcid.org/0000-0002-4779-7761,  
**S. Fischer**<sup>\*1</sup>,  
orcid.org/0000-0001-7298-9960

1 – Széchenyi István University, Győr, Hungary  
2 – Institute of Railway Systems and Public Transport, TU  
Dresden, Dresden, the Federal Republic of Germany  
3 – China Railway First Group Xinyun Engineering Co., Ltd,  
Xi'an, the People's Republic of China  
\* Corresponding author e-mail: [fischersz@sze.hu](mailto:fischersz@sze.hu)

## TESTING THE FRAGMENTATION OF RAILWAY BALLAST MATERIAL BY LABORATORY METHODS USING PROCTOR COMPACTOR

The physical classification of crushed stone and gravel used in railway construction is based on their strength and endurance and is performed by a laboratory test method using a rotating drum or a mortar method. The values of fracture resistance calculated using the Los Angeles method and abrasion calculated using the Micro-Deval method show a corresponding correlation and require further investigation.

**Purpose.** The development of a new method for measuring rock material fracture that is consistent with widely used standards while also being more comparable to real-world railway operating conditions. Certainly, both standard tests are essential for ensuring product homogeneity during production, so the new recommended method is only a supplement.

**Methodology.** The Proctor device was used to induce so-called shock loads from above, similar to railway loading conditions. Unlike the standard method, the andesite material was placed in a standard cylinder in these tests. The samples were pre-screened and sorted; the specified weight was approximately 1,300 g, and the specified sizes of the individual particles were 6.3, 8.0 and 11.2 mm. Only pre-washed and dried materials of NZ (fine crushed stone) or KZ (special crushed stone) from four different quarries (Tállya, Szob, Nógrád-kövesd, Recsk) with different rock physics characteristics were considered. The Proctor compactor machine was used because of its calculable labor (19.86 J/impact) and the crushing effect of the calculable impacts (64, 128, 256 and 1,028 blows). Even after loading different numbers of impacts, homogeneous samples from different quarries were sieved to measure the masses of fragments per fraction.

**Findings.** The set of measurements made it possible to establish a series of fragmentation and degradation curves for each of the three repeated measurements based on the composition of the material and the number of blows, which showed the degradation of samples with different physical and mechanical properties of the rock material and particle sizes. With an increasing number of impacts, the amount of crushed material in the sample increased, but the distribution of crushed material did not decrease evenly and proportionally as the number of impacts increased. Parameters and indices were also computed to identify various correlations (i. e.,  $F_V$ ,  $d < 22.4$ ,  $d < 0.5$ ,  $d < 0.063$  mm,  $C_U$ ,  $M$  ratio,  $\lambda$  ratio). Some of them (e. g.,  $F_V$ ) needed to be changed, but they were pre-defined due to the nature of the tests.

**Originality.** While many standard and alternative railway track ballast fragmentation test methods and measurement tools are available, this paper proposes a new laboratory method and demonstrates the specific measurement and application effectiveness.

**Practical value.** In addition to standard tests that are already widely used, the new method for measuring the fractional composition of railway ballast can help simulate real-world operating conditions of a railroad track in the laboratory. This method will improve the safety of railway operations.

**Keywords:** *railway track, ballasted track, material fractions, laboratory test, Proctor device*

**Introduction.** The most common railway superstructure in the world is the solution with tracks embedded in crushed stone. The static and dynamic loads transferred from the railway vehicles are transmitted to the rails via the railway wheelset, and these loads are further transmitted to the elements installed under the rails, such as the sleepers and the crushed stone ballast, which (last item) is the main subject of this article. The self-generating process of deterioration makes the rail ballast bed a transmitting element in the transfer and re-transfer of the loads coming from the vehicle, and any defects or uplift irregularities in the railway ballast will affect all elements of the load-bearing system. In case of inadequate maintenance/failure of any superstructure element, possible construction defects, and unevenness, the self-generating process of deterioration will accelerate. The basic principle of the process is shown in Fig. 1 [1].

Perhaps the least studied element of the process is the crushed-stone ballast, although this is the element with the most significant volume and mass in the cross-section of the railway track.

The deterioration of the ballast can have an impact on the life of the railway track, which various visible signs can manifest. The causes of ballast failure can be:

- non-compliance with construction technology (lower ballast, "mixing" sieving);
- contaminated crushed stone;
- ballast deficiencies (insufficient thickness of ballast layer or insufficient width of ballast shoulder);
- large-scale soil improvement layer installation (mixing sieving);
- operational deterioration (ballast fouling, crushing, sharp edge abrasion, wear, weed infestation, etc.);
- maintenance deficiencies.

The most common forms of deterioration are fragmentation (i.e., e.g., breakage) or abrasion, of which this article mainly deals with fragmentation. It is assumed that the effect of abrasion was significantly smaller, but these effects are most likely to occur together. Basically, the two concepts are difficult to distinguish, but the definition used in the research was that "fragmentation" meant the disintegration of a single grain into several parts, while wear meant the reduction of surface area, the rounding of grain shape. The qualification values from the

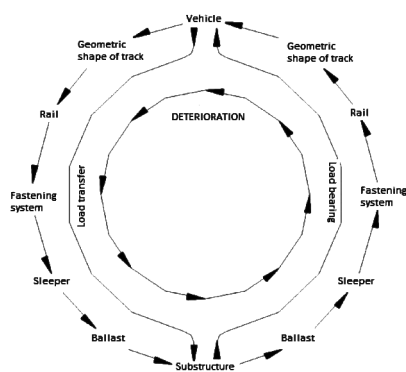


Fig. 1. The self-excitation process of deterioration

Los Angeles study attempt to characterize fragmentation more accurately, while the value from the Micro-Deval study attempts to characterize the wear phenomena more precisely.

**Standard tests.** In Hungary, crushed stone for railway track installation is covered by Government Decree 275/2013 (VII.16) [2], but as a product, it is classified as “road construction products”, while the conditions of use cover “all fields of application”. The Regulation provides for many tests to be carried out on aggregates, such as, but not limited to, the following rock classification tests:

- particle size distribution;
- fine grain content;
- particle shape;
- ...
- resistance to fragmentation;
- wear resistance.

Crushing, abrasion resistance, and classification into rock physics groups are carried out using two standard tests, both past and present, based on the current rock abrasion and impact abrasion tests (prescribed by [3]):

1. EN 1097-1:2011 Tests for mechanical and physical properties of aggregates – Part 1: Determination of the resistance to wear (micro-Deval) [4].
2. EN 1097-2:2020 Tests for mechanical and physical properties of aggregates – Part 2: Methods for the determination of resistance to fragmentation [5].

The principle of the tests also shows that the rock physics classification of crushed stones and gravels is based on their strength and durability properties. Determining the strength properties of such aggregate building stone materials is carried out in the regulatory systems of the various countries either by the rotary drum or mortar test method. In Hungary, all the product standards in force require one or more of the rotating drum tests to assess the suitability of the material for use.

Rock physics suitability tests are particularly important in the domestic certification practice. According to some experts, the Los Angeles test should retain its leading position in the future, but the test values can be compared with the test procedure developed to provide a broader view. For this reason, these values have been determined in advance for each quarry by an accredited metrology laboratory (NZ, KZ, where NZ means fine crushed stone, KZ means special crushed stone), from which the single-particle test materials have been separated and sieved to measure correlations.

The standard test methods are not comparable to real operating conditions, as the crushed stone grains are not abraded in a circular pattern when installed but have to withstand a distributed load from above. However, the two widely used standard tests, mandatory and/or recommended worldwide, are essential for manufacturing product consistency, and the test methods presented in this article can be used as a supplement.

**Literature review.** There is a large body of research on the subject, so a wide range of literature is available. There are also an extensive number of peer-reviewed journals on the study of

abrasion and fragmentation; however, in the area of transport engineering [6, 7], research is being carried out in almost all fields, from mining, rock physics, geology [8–10], mechanical and vehicle engineering [11], to architecture and civil engineering [12–14] and [15, 16], as well as logistics [17–19].

In general, for the fragmentation of the railway ballast, the following analytical methods are used by foreign researchers:

- laboratory tests;
- DEM (Discrete Element Method) simulations and/or 3D particle shape images;
- FEM (Finite Element Model) simulations;
- field (on track) tests.

The authors state several conclusions in the various literature, but it can be said that all the research results have been obtained because of the desire to improve the parameters of the ballast bed of the crushed stone or to understand the properties that have a particular impact on the life, aging, fragmentation.

There are still unknown parameters that complicate the research; for example, in a DEM simulation, the performance depends heavily on the calibration or the assignment of properties, but the shape of the particles depends on the contact force and the distribution [20]. Image-based procedures, such as 3D image analysis, are well suited for evaluating degradation, and several researchers are using the results to model maintenance cycles [21]. Both previous and current research on the subject of this article show that natural aggregates may have quite different properties according to their geologic origins and the production methods used at quarries. These materials were assembled using different ratios and constants in an attempt to characterize them as accurately as possible (F&E ratio – i. e., flat and elongated ratio –, AI – i. e., angularity index –, density), and the grain shape was also calculated, with flat and elongated grains breaking more typically at high densities [22]. Such constants and indexes are much needed because their creation and combination provide information that helps to determine better the value of the deterioration and, thus, the lifetime of the superstructures. The Los Angeles abrasion value has been shown to correlate closely with individually created compaction wear values and individual metrics, as the values obtained when implementing the modified compaction method, namely, the Compaction Abrasion Values (CAVs). The background to the test, as well as for the current study, was that the LA abrasion test, combined with the modified compaction test, used a similar treatment of the additives, namely grinding with steel balls and impacting with a compacting hammer [23].

**The purpose of the article** is to evaluate the results of the new laboratory test method, evaluating the results, looking for correlations between samples from different quarries. These results could provide baseline data to determine the lifetime of the ballasted track superstructure system and estimate the deterioration process. The long-term goal is to develop a measurement procedure predicting rail ballast fragmentation and replacement cycle time.

**Methods.** During the research, several types of laboratory tests were developed and conducted. There have been efforts to simulate the loads on the ballast in ways similar to in-service conditions and circumstances.

The test involved dynamically abrading a given amount of crushed stone loaded into a shear box [24].

The study involved a section of railway track in free space and was subjected to loading by a dynamic pulsator [25, 26].

In addition, small sets were loaded by a crusher in a hard polyethylene pipe plug. The loads were performed in steps, and an initial and intermediate computer tomography scan was taken for better evaluation or with discrete element modeling [27, 28].

In this section, all the studies referred to in the above paragraphs adhere to the methods used in the research, presented solely as a pre-history of the methods used in the current paper to keep track of the progress of the research.

The standard Proctor mold and the Proctor compactor machine were used to design the latest study.

The Proctor compactor machine was basically not used the same way as the standard Proctor test (EN 13286-2) [29]; only prewashed and dried particles were used in the testing mold and only for the calculable force.

- mold diameter – “A” ( $d_1$ ): 100 mm;
- mold height – “A” ( $h_1$ ): 120 mm;
- height of fall ( $h_2$ ): 457 mm;
- diameter of base ( $d_2$ ): 50 mm;
- mass of rammer – “B”: 4.50 kg;
- gravity acceleration: 9.81 m/s<sup>2</sup>;
- calculated impact surface:  $R^2 \cdot \pi = 0.0314 \text{ m}^2$ .

The force required to accelerate a tonne at m/s<sup>2</sup> is as follows.

Vehicle load: 225 kN = 22.5 tons·m/s<sup>2</sup> = 225,000 J/m

1 J = 1 N/m;

4.5 kg · 45 cm/100 · 9.81 m/s<sup>2</sup> = 19.87 J.

Load per area:

19.87 J/m = 19.87 · 0.001 kN;

19.87 J = 0.01987 kNm;

0.01987 kNm/0.0314 m<sup>2</sup> = 0.633 kN/m.

Specific energy carried out according to EN 13286-2 standard [29] is 0.342488 MJ/m<sup>3</sup> for 64 blows/layer.

When converting the value to kN, the “labor per area” value should be divided by the “calculated impact surface” value. It can be calculated that the number of axles “passed”, for which the converted values must be divided by 225 kN. “(the Zimmermann-Eisenmann calculation method needs to be considered in a detailed computation; the real, representative dynamic vertical load below a sleeper is approx. the one-third of 225 kN, i.e., 75.5 kN, in the case the design speed is 160 km/h and the quality of the track is appropriate).

Compaction energies and the number of axles calculated from it due to the number of blows are shown in Table 1.

The recalculated axle loads show that the number of stocks rolling over is still small, with a considerable value of axles rolling over in a relatively short time on a busy line. However, it can be concluded from the presented study that significant fines will appear even with a relatively small number of axles rolling through the railway ballast bed. The appearance of fine particles (and also dirt) does not necessarily indicate the need for replacement, but the extent of this is an important issue.

The test design is shown in Fig. 2.

Samples of andesite rock material from four quarries, which can be used for railway construction, were processed and provided by COLAS Északkő Kft.: Tállya, Szob, Nógrádkövesd, and Recsk.

For each quarry, the Los Angeles and Micro-Deval values per product were determined beforehand by an accredited metrology laboratory and are presented in Table 2.



Fig. 2. The test design

The samples were sorted, and homogeneous sets of three different grain sizes were created for each material from each quarry: 6.3, 8.0 and 11.2 mm particles. The original products were not used as mixed material on their own; occasionally, the mixing of single-grain samples from the same quarry was also applied for the laboratory tests.

In all cases, the particles were used in washed and dried conditions.

**The testing procedure.** The prepared samples of three different grain sizes were divided into 1,300 g (±5 g) sets. For each sample type, three sets were formed according to Table 3.

The weighed samples were loaded into the standard working test mold and then placed under the rammer head of the Proctor compactor machine. A 1,300 g sample of each particle size just filled the height of the standard cylindrical test mold. Due to the sudden impact of the rammer head, a height adjuster was used at the height of about 70 cm to prevent the particles from the pile from being thrown out of the pile, which

Table 1

Compaction energies due to the number of impacts

| No. of the blows | Specific energy according to standard, MJ/m <sup>3</sup> | Labor per area, kN/m <sup>2</sup> | Converted value to kN, kN | Calculated number of 225 kN axle load, pieces with a 75.5 kN vertical dynamic effect, pieces |
|------------------|--|-----------------------------------|---------------------------|--|
| 1                | 0.00535138   | 5.3514                            | 1,704.3                   | 22.6   |
| 64               | 0.34248816   | 342.4882                          | 109,072.7                 | 1,444.7  |
| 128              | 0.68497632   | 684.9763                          | 218,145.3                 | 2,889.3  |
| 256              | 1.36995263   | 1,369.9526                        | 436,290.6                 | 5,778.7  |
| 1024             | 5.47981054   | 5,479.8105                        | 1,745,162.6               | 23,114.7   |

Table 2

Los Angeles and Micro-Deval values according to [4, 5]

|          | Tállya (T)        |       | Szob (Sz) |       |
|----------|-------------------|-------|-----------|-------|
|          | LA                | MDE   | LA        | MDE   |
| KZ 4/8   | 17.71             | 8.90  | 16.03     | 18.07 |
| KZ 8/11  | 12.18             | 4.42  | 12.11     | 14.33 |
| KZ 11/16 | 14.04             | 3.42  | 12.14     | 13.65 |
|          | Nógrádkövesd (NK) |       | Recsk (R) |       |
|          | LA                | MDE   | LA        | MDE   |
| KZ 4/8   | 19.78             | 22.10 | 22.20     | 13.92 |
| KZ 8/11  | 16.58             | 18.30 | 17.46     | 10.42 |
| NZ 11/22 | 20.95             | 20.43 | 19.22     | 9.17  |

Table 3

Aggregation and the designation of samples

| Tálya (T)  | Szob (Sz)    | Nógrádkövesd (NK) | Recsk (R)   |
|--|--------------|-------------------|-------------|
| <b>6.3 mm grain size</b>                                 |              |                   |             |
| T-6.3/64   | Sz-6.3/64    | NK-6.3/64         | R-6.3/64    |
| T-6.3/128  | Sz-6.3/128   | NK-6.3/128        | R-6.3/128   |
| T-6.3/256  | Sz-6.3/256   | NK-6.3/256        | R-6.3/256   |
| T-6.3/1024   | Sz-6.3/1024  | NK-6.3/1024       | R-6.3/1024  |
| <b>8 mm grain size</b>                                   |              |                   |             |
| T-8/64   | Sz-8/64      | NK-8/64           | R-8/64      |
| T-8/128  | Sz-8/128     | NK-8/128          | R-8/128     |
| T-8/256  | Sz-8/256     | NK-8/256          | R-8/256     |
| T-8/1024   | Sz-8/1024    | NK-8/1024         | R-8/1024    |
| <b>11.2 mm grain size</b>                                |              |                   |             |
| T-11.2/64  | Sz-11.2/64   | NK-11.2/64        | R-11.2/64   |
| T-11.2/128   | Sz-11.2/128  | NK-11.2/128       | R-11.2/128  |
| T-11.2/256   | Sz-11.2/256  | NK-11.2/256       | R-11.2/256  |
| T-11.2/1024  | Sz-11.2/1024 | NK-11.2/1024      | R-11.2/1024 |
| <b>Altogether: 4 × 3 × 4 × 3 = 144 pieces of samples</b> |              |                   |             |

was fixed to the standard mold. This was replaced by a PVC pipe when the test was assembled, but a more durable metal elevating pipe was later manufactured.

The number of blows was determined this way because, during the impacting labor, the size of the rammer head did not cover the entire diameter of the mold. The standard compactor machine rotates the cylinder continuously at given angles after each stroke. The full circle was made in 8 strokes (with a uniform load), so multiples of 8 were determined.

For the number of blows, the numbers are given as a quadratic increase.

After each load (64, 128, 256 and 1,024 impacts/blows), the sample was disassembled as follows:

1. After loading, the sample was compressed (i.e., the original starting height relative to the top of the mold was reduced) due to the fragmentation of the sample, so these settlement values were measured.

2. The loaded sample pieces were placed in a standard sieve, and after sieving, the following fractions were weighed separately:

- 11.2 mm;
- 8.0 mm;
- 6.3 mm;
- 4.0 mm;
- 2.0 mm;
- 1.0 mm;
- 0.5 mm;
- 0.25 mm;
- 0.125 mm;
- 0.063 mm;
- 0.0 mm.

3. After the measurement, the test set was thrown in the trash and not used again for another measurement.

At least three measurements were executed from each homogeneous sample, and the mean values of these measurements for a given sample were considered. After each measurement, a new set was created.

**Standard deviation, relative standard deviation.** Fragmented parts were sieved to calculate the standard deviation and relative standard deviation. On this basis, the standard deviation and relative standard deviation values were calculated for the percentages of the parts broken off from the single-grain

Table 4

The values of the deviation and relative deviation of the broken-off particles (11.2 mm)

|                                | Number of the blows (11.2 mm) |       |       |       |
|--------------------------------|-------------------------------|-------|-------|-------|
|                                | 64                            | 128   | 256   | 1,024 |
| Average, %                     | 30.06                         | 36.72 | 42.43 | 60.59 |
| Standard deviation, %          | 12.27                         | 11.91 | 11.13 | 7.44  |
| Relative standard deviation, % | 40.81                         | 32.43 | 26.23 | 12.27 |

aggregate set. The values are shown in Table 4 (as an example for the 11.2 mm single grain aggregate). All types of single-grain aggregate (6.3, 8 and 11.2) sets behaved similarly.

The calculated standard deviation and relative standard deviation values showed that the variance between quarries varied between 7.44 and 12.27 %, but the relative standard deviation could be several times higher.

Table 4 also shows how the trends in the values compare. Both the standard deviation and the relative standard deviation decrease significantly with an increasing impact, so it can be said that the measurements become more accurate as the loads increase. All values change according to a linear

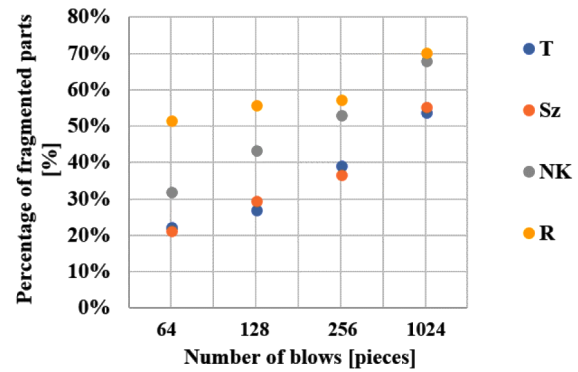


Fig. 3. Averages of sieved (fragmented) material 11.2 mm

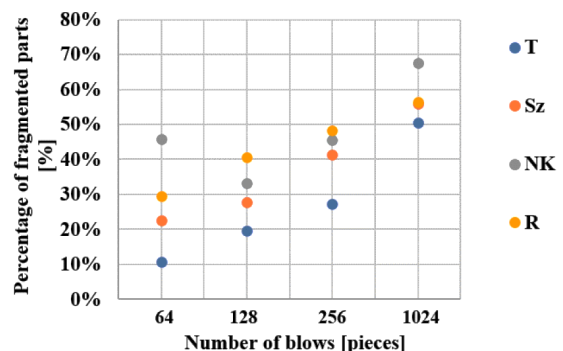
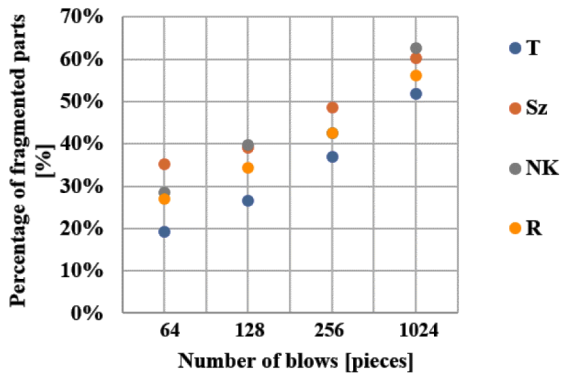


Fig. 4. Averages of sieved (fragmented) material 8 mm



| Number of blows | d=6.3 mm |        |        |        |
|-----------------|----------|--------|--------|--------|
|                 | T        | Sz     | NK     | R      |
| 64              | 19.22%   | 35.26% | 28.67% | 26.99% |
| 128             | 26.57%   | 39.12% | 39.74% | 34.37% |
| 256             | 37.07%   | 48.77% | 42.61% | 42.62% |
| 1024            | 51.86%   | 60.37% | 62.67% | 56.32% |

Fig. 5. Averages of sieved (fragmented) material 6.3 mm

function; the average values increase while the deviations decrease.

**Findings.** As expected from the design of the test method, every crushed stone particle set was highly fragmented after the impacts, the aim being to determine the exact size of the set per quarry and fraction as a function of the number of blows.

Figs. 3–5 show the rate of fragmentation, which is the percentage of the fraction of grains in a homogeneous cluster that became smaller than the initial size under different loads.

It can be seen that the average values recorded showed the most favorable properties for the andesite from the Tállya quarry, which produced the lowest fine ratios in all measurements. This is in accordance with the Los Angeles and Micro-Deval values obtained and, therefore, with the rock physics properties presented in Table 2.

The conclusions of the charts (Figs. 3–5) are detailed below:

1. In all but single grain size class, as the number of blows increased, so did the fines (the smaller grain sizes produced by the broken particles). In the case of the 8 mm set, samples from the Nógrádkövesd set were unique in disproving this increasing trend in the tests. Here, in fact, the clusters sampled at 64 blows showed the highest fragmentation.

2. For the 11.2 mm aggregates, the stone from Recsk showed the highest fragmentation value for each number of blows.

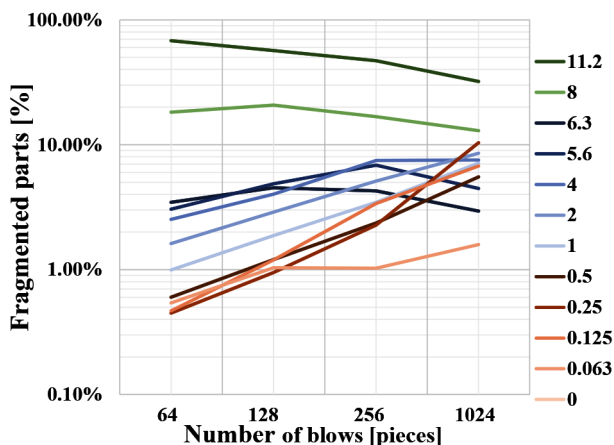


Fig. 6. Evolution of the fractions (Nógrádkövesd 11.2 mm)

3. For the 8 mm aggregates, the material from Nógrádkövesd showed the highest fines, but for the 6.3 mm aggregates, the material from Szob showed the same.

More exciting results were given by the evolution of the fractions, i.e., the distribution of the fragmented particles, which were compared based on the sieved volumes. Each example cannot be given here due to the large number of samples and the space limitations of this article.

The graph showing the evolution of the fractions (Fig. 6) as a trend was similar for all sets. The logarithmic curves clearly show that the larger particles gradually decrease, and the smaller ones increase. Half of the largest grain size of the pile is assumed to have a uniform fraction distribution during loading. The distributions increase gradually with the increasing number of blows for particle sizes smaller than half, as shown by the particle size distribution curve.

Fig. 7 demonstrates a typical particle size distribution curve (typical for all types of sets).

The assembled single-grain sets during the laboratory tests do not fall within the optimal limit curves in accordance with standards, either before or after fatigue. Knowing the initial size of each particle gave us a complete picture of the fragmentation by fraction and number of blows during the tests.

Even with the settlement value, it was self-evident that more blows would cause a higher settlement. However, the trends measured for the samples showed that the settlement showed a fit similar to a power function, as illustrated in the typical diagram and accompanied in Fig. 8. It is found that an exponential function can adequately approximate the vertical deformation of the samples. The compaction (settlement) of the larger grain size samples was the most significant, which can be explained by the higher initial void content. Thus, they suffered more significant vertical deformation with the applied fragmentation (crushing with Proctor compactor).

The measurements were also used to compare the properties of the size fraction with well-known constants that have been established by other researchers [30–32]:

- $F_V$  (%) (here, the authors considered  $F_V(AF)$ );
- $BBI$  (Ballast Breakage Index);
- $d < 22.4$ ,  $d < 0.5$ ,  $d < 0.063$  mm and their changes;
- $d_{60}/d_{10}$  ratio (the abbreviation  $C_U$  is applied);
- $MA$ ,  $MF$  and  $M_{avg}$  ( $A$  refers to lower, “ $F$ ” refers to the “upper” and “ $avg$ ” relates to the “average”);

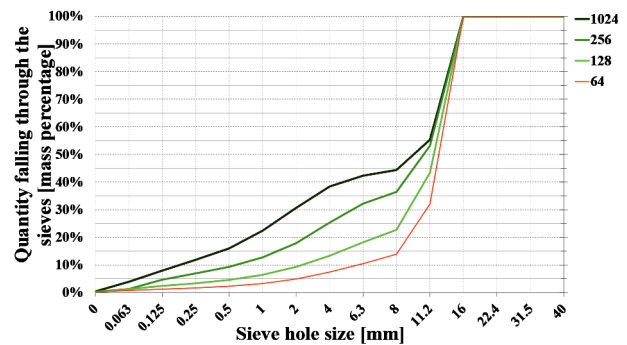


Fig. 7. Typical particle size distribution curves after fatigue ( $d = 11.2$  mm)

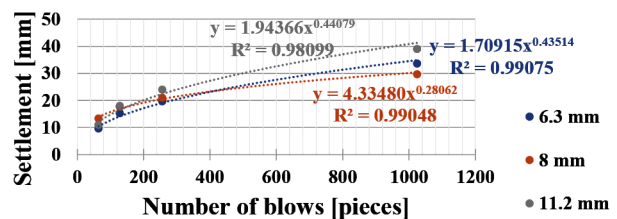


Fig. 8. Typical average values of settlement (Szob)

Table 6

Abrasion and degradation properties based on modified  $F_V(AF)$  values

| Modified $F_V(AF)$ values (after 1024 blows) |        |        |         |
|--|--------|--------|---------|
|  | 6.3 mm | 8 mm   | 11.2 mm |
| NK, %  | 100.00 | 100.00 | 100.00  |
| R, %   | 78.63  | 82.22  | 78.49   |
| Sz, %  | 70.69  | 71.83  | 84.38   |
| T, %   | 55.61  | 73.28  | 76.37   |

- $\lambda(AF)$ ;
- “AF” means after fatigue, “BF” means before fatigue.

While performing the calculations, it became apparent that since the aggregates were fatigued at homogeneous particle sizes, the initial starting values for many indexes were uninterpretable, and the calculation methods, which were tied to standard sieves, had to be modified to produce values based on the same principles but still usable. Using the above constants in their original form was impossible because of the computational and measurement constraints; however, we have tried to use calculation methods that are easily adaptable to current circumstances, with minor modifications.

The  $F_V$  value of the method used by the South African Railways is calculated according to the following formula [31]

$$F_V = (0.4 \cdot F_{19}) + (0.3 \cdot F_{6.7}) + (0.2 \cdot F_{1.18}) + (0.1 \cdot F_{0.15}),$$

where

$$F_{19} = (D_{19} \cdot 100)/27.0; \quad F_{6.7} = (D_{6.7} \cdot 100)/18.0;$$

$$F_{1.18} = (D_{1.18} \cdot 100)/11.5; \quad F_{0.15} = (D_{0.15} \cdot 100)/5.5.$$

The  $D_i$  values correspond to the mass percentage undersize the sieve size, i.e.,  $i$  (mm) (i.e., 19, 6.7, 1.18 and 0.15, respectively).

However, it was necessary to modify this slightly because the set used was single grain, and the grain size could not be applied similarly. The calculation method was retained in principle.

The particle size was determined by iteration, and the denominator was chosen to be the largest  $F_V(AF)$  value within the type set, as shown in Table 5 below. The most fragmented sets from which the divisors were derived are presented separately in Tables 7–9 (with 100 % value in the row corresponding to the  $F_V(AF)$ ).

Ballast screening becomes necessary if the original  $F_V \geq 80$  % [31]. Based on the value (metric) established, this can only be understood for “mixed” ballast used for railway construction, which is not homogeneous. The  $F_V(AF)$  values calculated with the modified constants and their trend lines are shown in Fig. 9. It has to be mentioned that there is a considered boundary condition  $F_V AF(0) = 0$  (i.e.,  $F_V(0) = 0$ ).

Several aggregates reached the 80 % limit, but these calculations differed significantly from the original formula. In the present document, the  $F_V(AF)$  value (a modified parameter in this case) has been adjusted to examine the relative fragmentation of the most fragmented aggregates.

Table 5

Calculation of  $F_V(AF)$  values for a given particle size

| Particle sizes and $F_V(AF)$ |                              |                              |
|------------------------------|------------------------------|------------------------------|
| 6.3 mm                       | 8 mm                         | 11.2 mm                      |
| $(D_{1.9} \cdot 100)/39.84$  | $(D_{2.41} \cdot 100)/43.90$ | $(D_{3.38} \cdot 100)/45.38$ |
| $(D_{0.67} \cdot 100)/26.85$ | $(D_{0.85} \cdot 100)/30.44$ | $(D_{1.19} \cdot 100)/33.30$ |
| $(D_{0.12} \cdot 100)/11.37$ | $(D_{0.15} \cdot 100)/13.29$ | $(D_{0.21} \cdot 100)/15.77$ |
| $(D_{0.015} \cdot 100)/1.29$ | $(D_{0.02} \cdot 100)/1.28$  | $(D_{0.03} \cdot 100)/1.17$  |

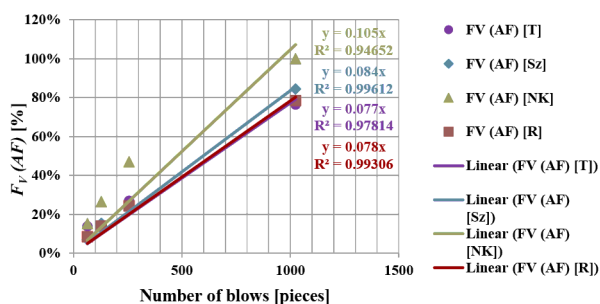


Fig. 9. The calculated  $F_V(AF)$  parameters ( $d = 11.2$  mm)

The most fragmentable rock material for all particle sizes was from N6gr6dk6vesd (the ratio is approx. 1.31, i.e. 0.105 : 0.08). Table 6, with the  $F_V(AF)$  values, shows the relative abrasion and degradation properties.

The measurements show that the  $F_V(AF)$  values correlate well with the fragmentation properties.

Relatively significant changes were required in calculating the  $BBI$  values, as the grain sizes of the original single grain set required a value of zero for the smaller sets so that no meaningful number could be obtained for the pre-fatigue values. As a result, many  $BBI$  values (especially at low impact rates) were negative. Correction for calculation inaccuracies due to homogeneous sets has not yet been made, so the results of these calculations are not included in this document.

The particle size distribution curves of ballast materials can be characterized by a pair of qualifying values and their average ( $MA$ ;  $MF$  or  $Mavg$ ) introduced for the particle size range 31.5–50 mm, by analogy with the fineness modulus used to characterize particle size distribution curves. The pair of qualifying values characterizing the entropy of ballast particles is the sum of the intercepts of the residual mass % at the lower and upper limit curves of the standard for the qualifying sieve sizes (22.5, 31.5, 40, 50 and 63 mm) [32].

The qualifying values generated could not be applied to a homogeneous set with a smaller grain size. A similar approach was taken here because the two adjacent standard sizes were selected for the ideal railroad ballast aggregate for particle sizes 31.5–50 mm. The neighbors of the standard sieve sizes associated with a given particle size were selected, and the remaining masses were tested for each test type:

- 6.3 mm: 8, 6.3, 4 mm sieves;
- 8 mm: 11.2, 8, 6.3 mm sieves;
- 11.2 mm: 16, 11.2, 8 mm sieves.

The ratios of the calculated modified  $MF$  values (the sum of the masses remaining on the given sieves after fatigue) to the  $MA$  values (essentially the total mass of the original sample – approx. 1,300 g) concerning the number of blows are shown in Fig. 10 (i.e.,  $M$  ratio values).

The presented  $M$  ratio values correlate well with the number of blows; the loaded samples from the four materials are correlated to logarithmic function approximations. While materials from three of the four quarries performed similarly, it is clear that the material from N6gr6dk6vesd shows the lowest  $M$

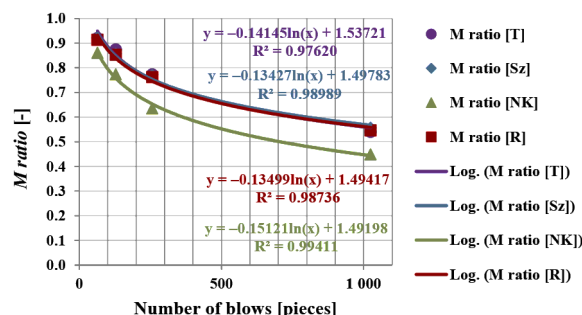


Fig. 10. The calculated  $M$  ratios ( $d = 11.2$  mm)

ratio values, and thus, these samples were the most prone to abrasion and fragmentation. The values start to deteriorate from about 0.9–0.95 and decrease to 0.55 after 1,024 blows in a logarithmic trend of deterioration. For the Nógrádkövesd andesite samples, which have exceptionally high LA and MDE values, these values start from 0.85 and decrease to 0.45 until the observed 1,024 blow value.

$M$  and  $\lambda$  values go “hand in hand”. The evaluation assumes that the previously installed crushed stone materials met the contemporary specifications for ballast materials with a grain size range of 31.5–50 mm.

The entropy of the aggregates placed in the pitch can be determined by the change in particle size distribution resulting from the test series. The change can be expressed by the change characteristic ( $\lambda$ ) for the qualifying mean value of the particle size distribution category “A” (qualifying average value is 253.5). Basically, it can be calculated as the  $M$  ratio values before and after fatigue to the qualifying average value. This calculation has been carried out, but the result shows a similar correlation with the  $M$  ratio values, which have a purely mathematical basis [32].

The calculated values and correlations of  $\lambda$  (AF) are shown in Fig. 11 in the case of  $d = 11.2$  mm. Similar observations can be made for  $\lambda$  (AF) and the  $M$  ratio.

Also, the authors had to change the values for the targeted particle sizes, i. e.,  $d < 22.4$  mm was not meaningful on any of the assembled sets. For an ideal railway ballast aggregate of 31.5–50 mm, the largest standard sieve size used was 63 mm (about a third of which was the 22.4 mm sieve), so to match the proportions, the 4 mm (also 0.5 and 0.063 mm) sieve was chosen for the 11.2 and 8 mm samples, furthermore 2.0, 0.25 and 0.063 mm sieves for the 6.3 mm samples.

The particle size fractions within the different sets were calculated; for example, the proportions of grain sizes of 4.0, 0.5 and 0.063 mm (in the case of 11.2 mm aggregate, but also similar to other aggregates) increased linearly with the load, as shown in Fig. 12. It is found that the most considerable increase in the amount of grains below 4 mm was in the 0–1,024 blow range (roughly 40 %; while those below 0.5 mm increased by

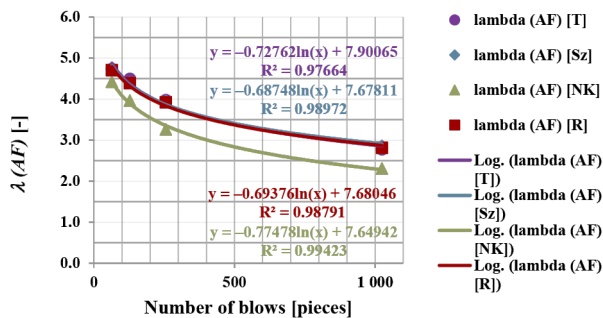


Fig. 11. The calculated  $\lambda$  (AF) values ( $d = 11.2$  mm)

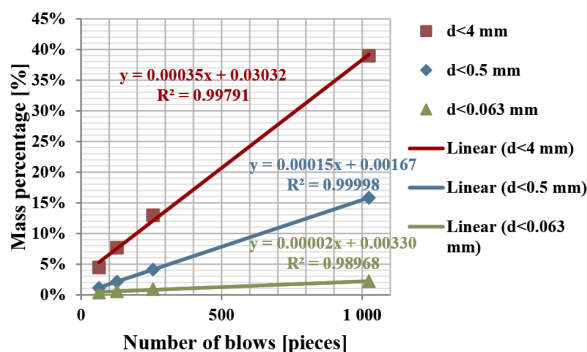


Fig. 12. Typical particle size fractions for a given size after the fatigue (Reck 11.2 mm)

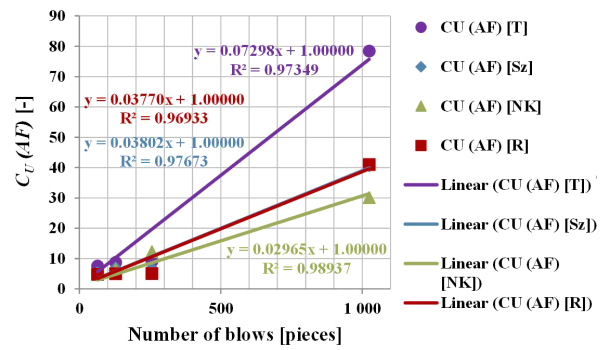


Fig. 13. The calculated  $C_V$  values ( $d = 11.2$  mm)

15 % and those below 0.063 mm by about 2.5 %), and the rate of increase (tangent) also showed a significant difference: compared to the slope of  $d < 0.063$  mm, the slope of the other two trend functions was 7.5 and 17.5 times, respectively.

Ways to characterize the particle size distribution include the uniformity coefficient ( $C_U$ ), which can be calculated using the formula  $d_{60}/d_{10}$ , where  $d_{60}$  is 60 % of the particle size and  $d_{10}$  is 10 %. Given that three different particle size set types were considered here, these values varied by test type:

1. 11.2 mm:  $d_{60} = 6.7$  mm,  $d_{10} = 1.1$  mm;
2. 8 mm:  $d_{60} = 4.8$  mm,  $d_{10} = 0.8$  mm;
3. 6.3 mm:  $d_{60} = 3.8$  mm,  $d_{10} = 0.63$  mm.

When examining the  $C_U$  values for all types of test samples (Fig. 13), linear regression functions are appropriate to approximate the deterioration trends. It has to be mentioned that there is a considered boundary condition  $C_U(0) = 1.0$  because the initial particle size distribution curves are vertical, i. e., the  $d_{60}/d_{10} = 1.0$ .

When all the characteristics are considered together, the  $LA$  and  $MDE$  values obtained and the calculated values confirm that aggregates from Reck and Nógrádkövesd are the most prone to fragmentation and abrasion. The parameters characterizing the crushed ballast particle fragmentation and the metrics indicating the need for ballast screening have been calculated, as shown in Tables 7–9.

Based on the values presented in Tables 7–9, the following conclusions can be drawn:

Table 7

Parameters characterizing the fragmentation for 6.3 mm sets

| Measured and calculated parameters                | Average of values measured on crushed stones (in proportion to the number of blows and the quarries) |           |                   |          |
|---|--|-----------|-------------------|----------|
|   | 6.3 mm homogeneous aggregates  |           |                   |          |
|   | Tállya (T)   | Szob (Sz) | Nógrádkövesd (NK) | Reck (R) |
| $LA$ , % – KZ 4/8                                 | 17.71  | 16.03     | 19.78             | 22.20    |
| $MDE$ , % – KZ 4/8                                | 8.90   | 18.07     | 22.10             | 13.92    |
| $LA + MDE$ , %                                    | 26.61  | 34.1      | 41.88             | 36.12    |
| $F_V$ (BF), %                                     | 0  | 0         | 0                 | 0        |
| $F_V$ (AF), %                                     | 64   | 10.21     | 11.50             | 12.77    |
|   | 128  | 16.93     | 14.05             | 20.69    |
|   | 256  | 27.31     | 26.13             | 38.63    |
|   | 1024   | 55.61     | 70.69             | 100.00   |
| Approximation curves (linear):                    |  |           |                   |          |
| T: $F_V( AF ) = 0.059 \cdot x$ , $R^2 = 0.92871$  |  |           |                   |          |
| Sz: $F_V( AF ) = 0.072 \cdot x$ , $R^2 = 0.97680$ |  |           |                   |          |
| NK: $F_V( AF ) = 0.102 \cdot x$ , $R^2 = 0.97734$ |  |           |                   |          |
| R: $F_V( AF ) = 0.082 \cdot x$ , $R^2 = 0.92287$  |  |           |                   |          |

|   |       |         |         |         |         |
|---|-------|---------|---------|---------|---------|
| $d < 2 \text{ mm } (AF), \%$  | 64    | 4.21    | 4.29    | 5.42    | 5.15    |
|   | 128   | 7.46    | 6.39    | 9.17    | 9.08    |
|   | 256   | 11.76   | 11.30   | 17.26   | 13.47   |
|   | 1,024 | 25.23   | 32.19   | 40.73   | 34.29   |
| $D < 0.25 \text{ mm } (AF), \%$   | 64    | 1.14    | 1.24    | 1.65    | 1.37    |
|   | 128   | 2.01    | 1.85    | 2.97    | 3.60    |
|   | 256   | 3.66    | 3.57    | 6.03    | 4.15    |
|   | 1,024 | 9.58    | 13.35   | 18.74   | 13.70   |
| $d < 0.063 \text{ mm } (AF), \%$  | 64    | 0.57    | 0.69    | 0.73    | 0.52    |
|   | 128   | 0.78    | 0.74    | 1.12    | 2.16    |
|   | 256   | 1.26    | 1.25    | 1.65    | 1.54    |
|   | 1,024 | 1.12    | 2.08    | 3.75    | 2.92    |
| $C_U(BF)$   |       | 1.00    | 1.00    | 1.00    | 1.00    |
| $C_U(AF)$   | 64    | 8.584   | 5.855   | 7.055   | 7.970   |
|   | 128   | 11.278  | 6.502   | 7.298   | 8.991   |
|   | 256   | 11.359  | 6.529   | 9.142   | 9.017   |
|   | 1,024 | 18.112  | 17.574  | 23.152  | 24.202  |
| Approximation curves (linear):<br>T: $C_U(AF) = 0.01937 \cdot x + 1.0, R^2 = 0.95445$<br>Sz: $C_U(AF) = 0.01710 \cdot x + 1.0, R^2 = 0.98002$<br>NK: $C_U(AF) = 0.02288 \cdot x + 1.0, R^2 = 0.99536$<br>R: $C_U(AF) = 0.02404 \cdot x + 1.0, R^2 = 0.98104$  |       |         |         |         |         |
| $M(BF)$   |       | 1,302.2 | 1,301.7 | 1,301.8 | 1,301.5 |
| $M(AF)$   | 64    | 1,211.6 | 1,196.4 | 1,180.2 | 1,188.7 |
|   | 128   | 1,155.9 | 1,151.1 | 1,099.9 | 1,122.0 |
|   | 256   | 1,076.9 | 1,042.1 | 959.5   | 1,026.1 |
|   | 1,024 | 880.8   | 768.6   | 667.1   | 760.9   |
| $M \text{ ratio}$   | 64    | 0.93    | 0.92    | 0.91    | 0.91    |
|   | 128   | 0.89    | 0.88    | 0.85    | 0.86    |
|   | 256   | 0.83    | 0.80    | 0.74    | 0.79    |
|   | 1,024 | 0.68    | 0.59    | 0.51    | 0.59    |
| Approximation curves (logarithmic):<br>T: $M \text{ ratio} = -0.09375 \cdot \ln(x) + 1.33397, R^2 = 0.98832$<br>Sz: $M \text{ ratio} = -0.12249 \cdot \ln(x) + 1.45660, R^2 = 0.96769$<br>NK: $M \text{ ratio} = -0.14525 \cdot \ln(x) + 1.53050, R^2 = 0.98809$<br>R: $M \text{ ratio} = -0.12051 \cdot \ln(x) + 1.43442, R^2 = 0.98025$ |       |         |         |         |         |
| $\lambda(BF)$   |       | 5.13    | 5.13    | 5.13    | 5.13    |
| $\lambda(AF)$   | 64    | 4.78    | 4.72    | 4.66    | 4.69    |
|   | 128   | 4.56    | 4.54    | 4.34    | 4.42    |
|   | 256   | 4.25    | 4.11    | 3.79    | 4.05    |
|   | 1,024 | 3.47    | 3.03    | 2.63    | 3.00    |
| Approximation curves (logarithmic):<br>T: $\lambda(AF) = -0.47885 \cdot \ln(x) + 6.83771, R^2 = 0.98691$<br>Sz: $\lambda(AF) = -0.62902 \cdot \ln(x) + 7.47984, R^2 = 0.96767$<br>NK: $\lambda(AF) = -0.74751 \cdot \ln(x) + 7.86832, R^2 = 0.98855$<br>R: $\lambda(AF) = -0.62005 \cdot \ln(x) + 7.37205, R^2 = 0.97996$                 |       |         |         |         |         |
| $\lambda \text{ ratio}$   | 64    | 0.93    | 0.92    | 0.91    | 0.91    |
|   | 128   | 0.89    | 0.88    | 0.85    | 0.86    |
|   | 256   | 0.83    | 0.80    | 0.74    | 0.79    |
|   | 1,024 | 0.68    | 0.59    | 0.51    | 0.59    |

Parameters characterizing the fragmentation for 8 mm sets

| Average of values measured on crushed stones<br>(in proportion to the number of blows and the quarries)   |  |           |                   |           |          |
|---|--|-----------|-------------------|-----------|----------|
| Measured and calculated parameters  | 8 mm homogeneous aggregates  |           |                   |           |          |
|   | Tálya (T)  | Szob (Sz) | Nógrádkövesd (NK) | Recsk (R) |          |
| $LA, \% - KZ 8/11$  | 12.18  | 12.11     | 16.58             | 17.46     |          |
| $MDE, \% - KZ 8/11$   | 4.42   | 14.33     | 18.30             | 10.42     |          |
| $LA + MDE, \%$  | 16.60  | 26.44     | 34.88             | 27.88     |          |
| $F_V(BF), \%$   | 0  | 0         | 0                 | 0         |          |
| $F_V(AF), \%$   | 64   | 10.60     | 8.27              | 11.54     | 8.44     |
|   | 128  | 17.64     | 21.69             | 18.38     | 14.93    |
|   | 256  | 28.98     | 24.09             | 35.41     | 29.78    |
|   | 1,024  | 73.28     | 71.83             | 100.00    | 82.22    |
|   | Approximation curves (linear):<br>T: $F_V(AF) = 0.075 \cdot x, R^2 = 0.96890$<br>Sz: $F_V(AF) = 0.073 \cdot x, R^2 = 0.96766$<br>NK: $F_V(AF) = 0.091 \cdot x + 0.07996, R^2 = 0.99490$<br>R: $F_V(AF) = 0.101 \cdot x, R^2 = 0.98647$ |           |                   |           |          |
| $d < 4 \text{ mm } (AF), \%$  | 64   | 4.95      | 5.52              | 8.02      | 5.73     |
|   | 128  | 9.70      | 9.78              | 12.02     | 10.04    |
|   | 256  | 15.72     | 15.62             | 23.01     | 19.27    |
|   | 1,024  | 37.33     | 38.90             | 49.99     | 42.70    |
| $d < 0.5 \text{ mm } (AF), \%$  | 64   | 1.38      | 1.31              | 2.12      | 1.40     |
|   | 128  | 2.68      | 3.14              | 3.53      | 2.83     |
|   | 256  | 5.08      | 4.56              | 7.37      | 5.85     |
|   | 1,024  | 16.90     | 16.04             | 24.89     | 19.21    |
| $d < 0.063 \text{ mm } (AF), \%$  | 64   | 0.66      | 0.44              | 0.59      | 0.40     |
|   | 128  | 0.89      | 1.42              | 0.96      | 0.67     |
|   | 256  | 1.20      | 1.26              | 1.38      | 1.49     |
|   | 1,024  | 2.47      | 3.08              | 3.23      | 3.01     |
| $C_U(BF)$   |  | 1.00      | 1.00              | 1.00      | 1.00     |
| $C_U(AF)$   | 64   | 3.581     | 5.262             | 4.072     | 3.926    |
|   | 128  | 4.528     | 5.801             | 6.055     | 4.798    |
|   | 256  | 7.215     | 6.418             | 8.757     | 7.176    |
|   | 1,024  | 28.991    | 32.326            | 36.879    | 47.606   |
| Approximation curves (linear):<br>T: $C_U(AF) = 0.02721 \cdot x + 1.0, R^2 = 0.99712$<br>Sz: $C_U(AF) = 0.03028 \cdot x + 1.0, R^2 = 0.97900$<br>NK: $C_U(AF) = 0.03488 \cdot x + 1.0, R^2 = 0.99668$<br>R: $C_U(AF) = 0.04405 \cdot x + 1.0, R^2 = 0.98662$  |  |           |                   |           |          |
| $M(BF)$   |  | 1,301.6   | 1,302.3           | 1,300.8   | 1,301.25 |
| $M(AF)$   | 64   | 1,173.3   | 1,179.2           | 1,100.4   | 1,148.8  |
|   | 128  | 1,063.6   | 1,094.5           | 1,047.7   | 1,056.1  |
|   | 256  | 964.1     | 980.8             | 877.7     | 912.2    |
|   | 1,024  | 737.8     | 726.6             | 572.9     | 688.2    |
| $M \text{ ratio}$   | 64   | 0.90      | 0.91              | 0.85      | 0.88     |
|   | 128  | 0.82      | 0.84              | 0.81      | 0.81     |
|   | 256  | 0.74      | 0.75              | 0.67      | 0.70     |
|   | 1,024  | 0.57      | 0.56              | 0.44      | 0.53     |
| Approximation curves (logarithmic):<br>T: $M \text{ ratio} = -0.12014 \cdot \ln(x) + 1.40187, R^2 = 0.99939$<br>Sz: $M \text{ ratio} = -0.12753 \cdot \ln(x) + 1.44944, R^2 = 0.99344$<br>NK: $M \text{ ratio} = -0.15275 \cdot \ln(x) + 1.51225, R^2 = 0.97641$<br>R: $M \text{ ratio} = -0.13037 \cdot \ln(x) + 1.43150, R^2 = 0.99640$ |  |           |                   |           |          |

|                         |   |      |      |      |      |
|-------------------------|---|------|------|------|------|
| $\lambda (BF)$          |   | 5.13 | 5.13 | 5.13 | 5.13 |
| $\lambda (AF)$          | 64  | 4.63 | 4.65 | 4.34 | 4.53 |
|                         | 128   | 4.20 | 4.32 | 4.13 | 4.17 |
|                         | 256   | 3.80 | 3.87 | 3.46 | 3.60 |
|                         | 1,024   | 2.91 | 2.87 | 2.26 | 2.71 |
|                         | Approximation curves (logarithmic):<br>T: $\lambda (AF) = -0.61778 \cdot \ln(x) + 7.20308, R^2 = 0.99944$<br>Sz: $\lambda (AF) = -0.62902 \cdot \ln(x) + 7.47984, R^2 = 0.96767$<br>NK: $\lambda (AF) = -0.74751 \cdot \ln(x) + 7.86832, R^2 = 0.98855$<br>R: $\lambda (AF) = -0.62005 \cdot \ln(x) + 7.37205, R^2 = 0.97996$ |      |      |      |      |
| $\lambda \text{ ratio}$ | 64  | 0.90 | 0.91 | 0.85 | 0.88 |
|                         | 128   | 0.82 | 0.84 | 0.81 | 0.81 |
|                         | 256   | 0.74 | 0.75 | 0.67 | 0.70 |
|                         | 1,024   | 0.57 | 0.56 | 0.44 | 0.53 |

Table 9

Parameters characterizing the fragmentation for 11.2 mm sets

| Average of values measured on crushed stones<br>(in proportion to the number of blows and the quarries) |  |           |                   |           |        |
|---|--|-----------|-------------------|-----------|--------|
| Measured and calculated parameters  | 11.2 mm homogeneous aggregates   |           |                   |           |        |
|   | Tálya (T)  | Szob (Sz) | Nógrádkövesd (NK) | Recsk (R) |        |
| LA, %<br>KZ 11/16, NZ 11/22   | 14.04  | 12.14     | 20.95             | 19.22     |        |
| MDE, %<br>KZ 11/16, NZ 11/22  | 3.42   | 13.65     | 20.43             | 9.17      |        |
| LA + MDE, %   | 17.46  | 25.79     | 41.38             | 28.39     |        |
| $F_V(BF)$ , %   | 0  | 0         | 0                 | 0         |        |
| $F_V(AF)$ , %   | 64   | 13.85     | 6.95              | 15.14     | 8.42   |
|   | 128  | 13.51     | 15.39             | 26.52     | 14.00  |
|   | 256  | 26.97     | 23.59             | 46.97     | 24.33  |
|   | 1,024  | 76.37     | 84.38             | 100.00    | 78.49  |
|   | Approximation curves (linear):<br>T: $F_V(AF) = 0.077 \cdot x, R^2 = 0.97814$<br>Sz: $F_V(AF) = 0.084 \cdot x, R^2 = 0.99612$<br>NK: $F_V(AF) = 0.105 \cdot x, R^2 = 0.94652$<br>R: $F_V(AF) = 0.078 \cdot x, R^2 = 0.99306$ |           |                   |           |        |
| $d < 4 \text{ mm}$<br>(AF), %   | 64   | 4.77      | 3.97              | 7.41      | 4.45   |
|   | 128  | 7.72      | 8.17              | 13.32     | 7.68   |
|   | 256  | 14.27     | 13.20             | 25.33     | 12.95  |
|   | 1,024  | 41.31     | 38.40             | 47.71     | 38.97  |
| $d < 0.5 \text{ mm}$<br>(AF), %   | 64   | 1.49      | 0.87              | 2.28      | 1.11   |
|   | 128  | 1.88      | 2.24              | 4.56      | 2.13   |
|   | 256  | 4.20      | 3.79              | 9.30      | 4.11   |
|   | 1,024  | 15.70     | 16.00             | 24.58     | 15.81  |
| $d < 0.063 \text{ mm}$<br>(AF), %   | 64   | 0.87      | 0.29              | 0.77      | 0.36   |
|   | 128  | 0.53      | 0.67              | 1.21      | 0.56   |
|   | 256  | 1.04      | 1.00              | 1.29      | 0.92   |
|   | 1,024  | 1.29      | 3.89              | 2.00      | 2.19   |
| $C_U(BF)$   | 1.00   | 1.00      | 1.00              | 1.00      |        |
| $C_U(AF)$   | 64   | 7.561     | 5.297             | 4.780     | 4.825  |
|   | 128  | 8.724     | 6.882             | 6.530     | 5.017  |
|   | 256  | 9.144     | 6.779             | 12.291    | 5.046  |
|   | 1,024  | 78.449    | 40.674            | 30.105    | 41.018 |

|  |   |         |         |         |         |
|--|---|---------|---------|---------|---------|
| Approximation curves (linear):<br>T: $C_U(AF) = 0.07298 \cdot x + 1.0, R^2 = 0.97349$<br>Sz: $C_U(AF) = 0.03802 \cdot x + 1.0, R^2 = 0.97673$<br>NK: $C_U(AF) = 0.02965 \cdot x + 1.0, R^2 = 0.98937$<br>R: $C_U(AF) = 0.03770 \cdot x + 1.0, R^2 = 0.96933$ |   |         |         |         |         |
| $M(BF)$  |   | 1,301.7 | 1,300.8 | 1,301.0 | 1,303.3 |
| $M(AF)$  | 64  | 1,199.3 | 1,200.2 | 1,120.0 | 1,191.5 |
|  | 128   | 1,138.7 | 1,115.2 | 1,004.7 | 1,111.4 |
|  | 256   | 1,006.6 | 1,001.4 | 826.7   | 993.4   |
|  | 1,024   | 703.3   | 724.2   | 584.7   | 712.8   |
| $M \text{ ratio}$  | 64  | 0.92    | 0.92    | 0.86    | 0.91    |
|  | 128   | 0.87    | 0.86    | 0.77    | 0.85    |
|  | 256   | 0.77    | 0.77    | 0.64    | 0.76    |
|  | 1,024   | 0.54    | 0.56    | 0.45    | 0.55    |
|  | Approximation curves (logarithmic):<br>T: $M \text{ ratio} = -0.14145 \cdot \ln(x) + 1.53721, R^2 = 0.97620$<br>Sz: $M \text{ ratio} = -0.13427 \cdot \ln(x) + 1.49783, R^2 = 0.98989$<br>NK: $M \text{ ratio} = -0.15121 \cdot \ln(x) + 1.49198, R^2 = 0.99411$<br>R: $M \text{ ratio} = -0.13499 \cdot \ln(x) + 1.49417, R^2 = 0.98736$ |         |         |         |         |
| $\lambda (BF)$   |   | 5.13    | 5.13    | 5.13    | 5.13    |
| $\lambda (AF)$   | 64  | 4.73    | 4.73    | 4.42    | 4.70    |
|  | 128   | 4.49    | 4.40    | 3.96    | 4.38    |
|  | 256   | 3.97    | 3.95    | 3.26    | 3.92    |
|  | 1,024   | 2.77    | 2.86    | 2.31    | 2.81    |
|  | Approximation curves (logarithmic):<br>T: $\lambda (AF) = -0.72762 \cdot \ln(x) + 7.90065, R^2 = 0.97664$<br>Sz: $\lambda (AF) = -0.68748 \cdot \ln(x) + 7.67811, R^2 = 0.98972$<br>NK: $\lambda (AF) = -0.77478 \cdot \ln(x) + 7.64927, R^2 = 0.99423$<br>R: $\lambda (AF) = -0.69376 \cdot \ln(x) + 7.68046, R^2 = 0.98791$             |         |         |         |         |
| $\lambda \text{ ratio}$  | 64  | 0.92    | 0.92    | 0.86    | 0.91    |
|  | 128   | 0.87    | 0.86    | 0.77    | 0.85    |
|  | 256   | 0.77    | 0.77    | 0.64    | 0.76    |
|  | 1,024   | 0.54    | 0.56    | 0.45    | 0.55    |

1. The  $\lambda (BF)$  and  $M \text{ ratio}$  (for before fatigue) values are constant over the whole test series, with approx. 1,300 and 5.13, respectively.

2. A clear and strong correlation with the value of the blow number was observed for all parameters. Typically, linear or logarithmic regression functions could be defined.

3. For mathematical reasons, the calculated  $\lambda (AF)$  and  $M \text{ ratio}$  values are similar and follow a logarithmic trend with increasing load.

4. The  $F_V(AF)$  and  $C_U(AF)$  values follow a linear trend with increasing load in all cases.

5. For materials from quarries Tálya (T), Szob (Sz) and Recsk (R) (andesite), the deterioration functions could be described by similar regression functions. The notable exception in all cases was the NK (quarry Nógrádkövesd) material for all fractions, presumably due to its worse rock physics, i.e., the highest fragmentation properties (LA and MDE values in Tables 2 and 7–9).

It can be concluded that a more detailed analysis is definitely needed in terms of how exactly the deterioration trends depend on the LA, MDE, and possibly LA + MDE parameters.

**Originality.** Several standard and alternative test methods for determining rail ballast fragmentation (breakage) exist. Several researchers have attempted to develop different measurement techniques, as evidenced by literature surveys. In our country, the lack of funding for research does not necessarily allow the same conditions as in foreign universities. The Proc-

tor compactor machine, used for soil testing, was used as the basic measuring instrument available for the provision, thus diversifying the research methods. The method developed here has been used in this form before, but the assembled sets were not loaded at this impact rate, and the material was not andesite, so essentially, an additional measurement was developed [9]. In addition, it should be pointed out that the test is dynamic, which is even closer to the operating conditions and, therefore, more effective than a series of static laboratory tests.

In any case, it should be pointed out that the grain samples examined are, on the one hand, scaled down. This means that instead of the 31.5/50 or 31.5/63 mm products typical of railway ballast, 4/8, 8/11, 11/16 and 11/22 mm crushed stones were tested under laboratory conditions (more specifically, the 6.3, 8.0 and 11.2 mm fractions were sieved from these products and only these three fractions were tested from each product from the different quarries). It should be noted that samples for testing were also taken from the same explosive stockpile from each quarry (all of the quarries contain andesite rock). In addition, conventional 31.5/50 mm product from the identical (same) production batches was also set aside to ensure that the rock physics characteristics were known for a subsequent detailed or additional series of tests.

**Practical value.** In the current series of experiments, the primary aim was to apply and test an alternative laboratory dynamic test method that is relatively simple, cheap, and easily accessible. The Proctor compactor, used in geotechnical soil testing, was found to be the most suitable for this purpose. The basic idea was to be able to investigate rocks from which, in practice, a conventional size (31.5/50 and/or 31.5/63 mm) railway crushed stone ballast could be produced daily. For this purpose, four opencast quarries of Colas Északkő Kft. were designated: Tállya, Szob, Nógrádkövesd, as well as Recsk. As the original unmodified Proctor compaction container (cylinder) is not suitable for measuring crushed stones of this grain size, samples of reduced grain size were tested: 4/8, 8/11, 11/16 and 11/22 mm products. The 6.3, 8.0 and 11.2 mm fractions were sieved from these crushed products. In each case, a sample of approximately 1,300 g was loaded into the cylinder. For each fraction, 64, 128, 256 and 1,024 blows were used to compact the samples, i. e., to crush them more precisely (this was called fatigue). The exact particle size distribution of each sample was then measured. Each measurement was repeated three times, resulting in 144 measurements. Various shape parameters were determined from the grain distribution curves of the samples after fatigue. A strong correlation was found for all of them as a function of the number of blows. In the case of the andesite from Nógrádkövesd quarry, which has less favorable rock physics, significant differences were observed in the amount of crushed material and the absolute value of some shape parameters (after fatigue), as well as in the rate of deterioration. Products from the other three quarries gave roughly similar results.

The authors proved that the new measurement method can help simulate real operating conditions under laboratory conditions to complement the application of widely used standard tests. Experience has shown that the measurements correlate well with all known characteristics, so it is well suited to serve as an additional measurement to determine the breakage behavior of crushed aggregates.

Based on the shown and detailed analysis, it can be stated that a deeper examination of how exactly the deterioration trends depend on the *LA*, *MDE*, and possibly *LA + MDE* parameters is required. The modified *BBI* parameter is also recommended to consider.

It would be preferable if generalizations could be made from the detailed analysis, making it possible to avoid using or even omitting rock physics features. It is known that there are several countries that, for example, do not require maximum Micro-Deval values for their railway ballast material, and their Los Angeles crushing requirements are considerably more relaxed and lenient than those of the Hungarian State Railways

(MÁV). In 2023, a six-member technical committee developed the MÁV Instruction D.26, which has not yet been implemented and has not yet become legally enforced. In it, recommendations and specifications were made which, according to the current body of knowledge and professional experience, are the most favorable for the production, transport, installation, operation, and maintenance of crushed stone.

The authors propose to continue in the direction of research outlined above.

## References.

- Horvát, F. (2015). *Mérnöki módszerek III.* Széchenyi István University. Győr.
- Internet law library (2023, October 31). Retrieved from <https://net.jogtar.hu/jogszabaly?docid=a1300275.kor>.
- European Committee for Standardization (2012). *Aggregates for railway ballast* (EN 13450). Retrieved from <https://standards.iteh.ai/catalog/standards/cen/c05b9399-6075-42e0-9274-28742fa20327/en-13450-2013>.
- European Committee for Standardization (2012). *Tests for mechanical and physical properties of aggregates – Part 1: Determination of the resistance to wear (micro-Deval)* (EN 1097-1). Retrieved from <https://standards.iteh.ai/catalog/standards/cen/0704a937-7494-49be-827a-1da432fc0024/en-1097-1-2011>.
- European Committee for Standardization (2020). *Tests for mechanical and physical properties of aggregates – Part 2: Methods for the determination of resistance to fragmentation* (EN 1097-2). Retrieved from <https://standards.iteh.ai/catalog/standards/cen/2b59008c-ab4d-428f-9e85-780705498a57/en-1097-2-2020>.
- Kurhan, M. B., Kurhan, D. M., Husak, M. A., & Hmelevska, N. (2022). Increasing the efficiency of the railway operation in the specialization of directions for freight and passenger transportation. *Acta Polytechnica Hungarica*, 19(3), 231-244. <https://doi.org/10.12700/APH.19.3.2022.3.18>.
- Gáspár, L., Horvát, F., & Lublós, L. (2011). *Lifetime of transport infrastructure facilities.* Universitas-Győr Nonprofit Kft., Győr.
- Czinder, B., Vásárhelyi, B., & Török, Á. (2021). Long-term abrasion of rocks assessed by micro-Deval tests and estimation of the abrasion process of rock types based on strength parameters. *Engineering Geology*, 282, 105996. <https://doi.org/10.1016/j.enggeo.2021.105996>.
- Shehu, S. A., Yusuf, K. O., Zabidi, H., Jimoh, O. A., & Hashim, M. H. M. (2023). Blasting efficiency in granite aggregate quarry based on the combined effects of fragmentation and weighted environmental hazards. *Mining of Mineral Deposits*, 17(1), 120-128. <https://doi.org/10.33271/mining17.01.120>.
- Haddad, J., Alfaqs, F., Al-quraan, T., & Ikhries, I. I. (2023). Investigation of vibrating jaw crusher experimental variables. *Mining of Mineral Deposits*, 17(3), 49-55. <https://doi.org/10.33271/mining17.03.049>.
- Taran, I., & Klymenko, I. (2017). Analysis of hydrostatic mechanical transmission efficiency in the process of wheeled vehicle braking. *Transport Problems*, 12(Special Edition), 45-56. <https://doi.org/10.20858/tp.12.se.4>.
- Kurhan, D. M. (2023). Entropy Application for Simulation the Ballast State as a Railway Element. *Acta Polytechnica Hungarica*, 20(1), 63-77. <https://doi.org/10.12700/APH.20.1.2023.20.5>.
- Kurhan, M. B., Kurhan, D. M., Husak, M. A., & Hmelevska, N. (2022). Development of the High-Speed Running of Trains in Ukraine for Integration with the International Railway Network. *Acta Polytechnica Hungarica*, 19(3), 207-218. <https://doi.org/10.12700/APH.19.3.2022.3.16>.
- Károlyfi, K. (2017). The effect of saturation degree of cement paste on fair-faced concrete surfaces. *Építőanyag (Online)*, (2), 55. <https://doi.org/10.14382/epitoanyag-jsbcm.2017.10>.
- Kuchak, A. J. T., Marinkovic, D., & Zehn, M. (2020). Finite element model updating – Case study of a rail damper. *Structural Engineering and Mechanics*, 73(1), 27-35. <https://doi.org/10.12989/sem.2020.73.1.027>.
- Kuchak, A. J. T., Marinkovic, D., & Zehn, M. (2021). Parametric Investigation of a Rail Damper Design Based on a Lab-Scaled Model. *Journal of Vibration Engineering and Technologies*, 9(1), 51-60. <https://doi.org/10.1007/s42417-021-00341-7>.
- Taran, I., & Bondarenko, A. (2017). Conceptual approach to select parameters of hydrostatic and mechanical transmissions for wheel tractors designed for agricultural operations. *Archives of transport*, 41(1), 89-100. <https://doi.org/10.5604/01.3001.0009.7389>.
- Saukenova, I., Oliskeych, M., Taran, I., Toktamyssova, A., Aliakbarkyzy, D., & Pelo, R. (2022). Optimization of schedules for

early garbage collection and disposal in the megapolis. *Eastern-European Journal of Enterprise Technologies*, 1(3-115), 13-23. <https://doi.org/10.15587/1729-4061.2022.251082>.

19. Taran, I., & Litvin, V. (2018). Determination of rational parameters for urban bus route with combined operating mode. *Transport Problems*, 13(4), 157-171. <https://doi.org/10.20858/tp.2018.13.4.14>.
20. González, J. I., & Salazar, F. (2018). Advances in the modelling of railway ballast using the Discrete Element Method (DEM). *The Fourth International Conference on Railway Technology, presentation*. Retrieved from <https://www.researchgate.net/publication/328042347>.
21. Guo, Y., Markine, V., Song, J., & Jing, G. (2018). Ballast degradation: Effect of particle size and shape using Los Angeles Abrasion test and image analysis. *Elsevier, Construction and Building Materials*, 169, 414-424. <https://doi.org/10.1016/j.conbuildmat.2018.02.170>.
22. Wnek, M. A., Tutumluer, E., Moaveni, M., & Gehringer, E. (2013). Investigation of Aggregate Properties Influencing Railroad Ballast Performance. *Journal of the Transportation Research Board*, (2374), 180-189. <https://doi.org/10.3141/2374-21>.
23. Mohajerani, A., Nguyen, B. T., Tanriverdi, Y., & Chandrawanka, K. (2017). A new practical method for determining the LA abrasion value for aggregates. *Elsevier B. V., Soils and Foundations*, 57, 840-848. <https://doi.org/10.1016/j.sandf.2017.08.013>.
24. Fischer, S. (2023). Evaluation of inner shear resistance of layers from mineral granular materials. *Facta Universitatis, Series: Mechanical Engineering*. <https://doi.org/10.22190/FUME230914041F>.
25. Szalai, S., Eller, B., Juhász, E., Movahedi Rad, M., Németh, A., Harrach, D., Baranyai, G., & Fischer, Sz. (2022). Investigation of deformations of ballasted railway track during collapse using the Digital Image Correlation Method (DICM). *Reports in Mechanical Engineering*, 3(1), 258-282. <https://doi.org/10.31181/rme20016032022s>.
26. Juhász, E., Movahedi Rad, M., Fekete, I., & Fischer, S. (2019). Discrete element modelling of particle degradation of railway ballast material with PFC3D software. *Nauka ta Progres Transportu*, 6(84), 103-116. <https://doi.org/10.15802/stp2019/194472>.
27. Jia, W., Markine, V., & Guo, Y. (2023). Efficiency analysis and optimisation of DEM for railway ballast track simulations: Multi-layer shape model of lateral resistance. *Transportation Geotechnics*, 40, 100977. <https://doi.org/10.1016/j.trgeo.2023.100977>.
28. Lu, M., & McDowell, G. R. (2007). The importance of modelling ballast particle shape in the discrete element method. *Granular Matter*, 9(1-2), 69-80. <https://doi.org/10.1007/s10035-006-0021-3>.
29. European Committee for Standardization (2012). *Unbound and hydraulically bound mixtures. Part 2: Test methods for laboratory reference density and water content. Proctor compaction* (EN 13286-2:2010/AC:2012). Retrieved from <https://standards.iteh.ai/catalog/standards/cen/5b4df027-90e4-4ccd-a119-e6ac12b80cd1/en-13286-2-2010-ac-2012>.
30. Indraratna, B., Salim, W., & Rujikiatkamjorn, C. (2011). Advanced rail geotechnology – Ballasted track. *CRC Press Taylor & Francis Group*, London. ISBN 978-0-415-66957-3.
31. Lichtberger, B. (2005). *Track compendium*. Hamburg: Eurailpress Tetzlaff-Hestra GmbH & Co. KG.
32. Gálos, M., Kárpáti, L., & Szekeres, D. (2011). Ágyazati kőanyagok. A kutatás eredményei (2. rész). *Sínek Világa*, 53(1), 6-13. Retrieved from [https://www.sinekvilaga.hu/documents/2011\\_1.pdf](https://www.sinekvilaga.hu/documents/2011_1.pdf).

## Тестування фракційного складу залізничного баласту лабораторними методами з використанням пристрою Проктора

Е. Гушек-Юхаш<sup>1</sup>, А. Немес<sup>1</sup>, М. Сисун<sup>2</sup>, Г. Бараняй<sup>1</sup>,  
Я. Лю<sup>3</sup>, Ш. Фішер<sup>\*1</sup>

- 1 – Університет Сечені Іштвана, м. Д'єр, Угорщина
  - 2 – Інститут залізничних систем і громадського транспорту, ТУ Дрезден, м. Дрезден, Федеративна Республіка Німеччина
  - 3 – Китайська залізниця Перша група Xinyun Engineering Co., м. Сіань, Китайська Народна Республіка
- \* Автор-кореспондент е-mail: [fischersz@sze.hu](mailto:fischersz@sze.hu)

Фізична класифікація подрібненого щебню та гравію, що використовується в будові залізничної колії, ґрунтується на їх міцності й витривалості та виконується за допомогою лабораторного тестового методу, використовуючи барабан, який обертається, або метод мортири. Значення стійкості до руйнування за методом Лос-Анджелеса та стирання за методом Мікро-Деваля демонструють відповідну кореляцію й потребують подальшого вивчення.

**Мета.** Розробка нового методу вимірювання руйнування матеріалу гірських порід, який має відповідність з відомими стандартами, що мають широке застосування, а також є більш порівнянним із реальними умовами експлуатації залізниці. Звісно, обидва стандартні тести є невід'ємними для забезпечення однорідності продукту під час виробництва, тому новий рекомендований метод є лише доповненням.

**Методика.** За допомогою пристрою Проктора були індуковані ударні навантаження зверху, схожі на умови залізничного навантаження. На відміну від стандартного методу, у цих випробуваннях матеріал андезиту поміщали до стандартного циліндру. Зразки були попередньо просіяні й відсортовані; задана вага становила приблизно 1300 г, а задані розміри окремих часток становили 6.3, 8.0 та 11.2 мм. Розглядалися лише попередньо промиті й висушені матеріали NZ (дрібний щебін) або KZ (спеціальний щебін) із чотирьох різних кар'єрів (Tállya, Szob, Nógrádkövesd, Recsk) з різними фізико-механічними характеристиками порід. Пристрій Проктора використовували через його розрахункову дію (19,86 Дж/удар) і розрахунковий вплив різної кількості ударів (64, 128, 256, 1028 ударів). Після навантаження різної кількості ударів однорідні зразки з різних кар'єрів просіювали для вимірювання маси фрагментів кожної фракції.

**Результати.** Серія вимірювань дала можливість встановити за складом матеріалу й кількістю ударів ряд критичних фрагментації та деградації для кожного з трьох повторних вимірювань, що показали деградацію зразків з різними фізико-механічними властивостями матеріалу гірських порід і розмірами часток. Зі збільшенням кількості ударів кількість подрібненого матеріалу у зразку зростала, але розподіл подрібненого матеріалу не зменшувався рівномірно й пропорційно зі збільшенням кількості ударів. Вертикальна деформація зразків збільшувалася як функція сили. Також були розраховані параметри та індекси для виявлення різних кореляцій (тобто,  $F_V$ ,  $d < 22.4$ ,  $d < 0.5$ ,  $d < 0.063$  mm,  $C_V$ ,  $M$  ratio,  $\lambda$  ratio). Деякі з них довелося модифікувати (наприклад,  $FV$ ), але вони були заздалегідь визначені через специфіку

**Наукова новизна.** Хоча існує багато стандартних і альтернативних методів випробувань на фрагментацію баласту залізничної колії та засобів вимірювання, у роботі запропоновано новий лабораторний метод і було продемонстроване конкретне вимірювання та ефективність його застосування.

**Практична значимість.** Новий метод вимірювання фракційного складу залізничного баласту може допомогти моделювати в лабораторії реальні робочі умови функціонування залізничної колії, щоб доповнити стандартні тести, які вже мають широке використання. Цей метод підвищить безпечність роботи залізниці.

**Ключові слова:** залізнична колія, баластна колія, фракції матеріалу, лабораторне випробування, пристрій Проктора

*The manuscript was submitted 08.08.23.*